Direct Determination of Surface Albedos from Satellite Imagery

YURI MEKLER AND JOACHIM H. JOSEPH[1]

Department of Geophysics and Planetary Sciences, Tel-Aviv University, Ramat Aviv, Israel

(Manuscript received 3 November 1981, in final form 23 November 1982)

ABSTRACT

An empirical method to measure the spectral surface albedo of surfaces from LANDSAT imagery is presented and analyzed.

The empiricism in the method is due only to the fact that three parameters of the solution must be determined for each spectral photograph of an image on the basis of independently known albedos at three points. The approach is otherwise based on exact solutions of the radiative transfer equation for upwelling intensity.

Application of the method allows the routine construction of spectral albedo maps from satellite imagery, without requiring detailed knowledge of the atmospheric aerosol content, as long as the optical depth is less than 0.75, and of the calibration of the satellite sensor.

1. Introduction

The possibility of detailed analysis of the Earth's surface from satellite altitudes is one of the recent important advances in many disciplines—from climate and weather studies through the remote mapping of earth resources to military applications.

One of the basic steps in the analysis is the determination of the true spectral reflectivity of the surface from the image. This determination depends on the required resolution or on the size of the surface element, on atmospheric properties and on the detecting system.

In this paper we suggest an empirical approach to this problem. The approach is firmly based on exact radiative transfer theory and its errors and application are explored here.

In Section 2 we derive our approximation to the exact monochromatic solution for upwelling nadir intensity and assess the error and the validity of the basic assumptions necessary. In Section 3, we present the spectrally integrated form of our approach. Section 4 describes the experimental determination of the three parameters, and in Section 5 we outline the application to satellite data. Section 6 summarizes our suggestions.

2. The approximation to the exact solution

The exact monochromatic solution of the radiative transfer equation for the upward intensity over a homogeneous terrain with Lambertian albedo A is

$$I^A = I^0 + \frac{GA}{1 - LA}, \tag{1}$$

where I^0 is the upward intensity for the case of a black ($A = 0$) surface, and G and L are functions of the optical depth δ (Chandrasekhar 1960; Sobolev, 1975).

This equation is strictly valid for the case of a plane-parallel atmosphere overlying a plane reflecting surface with an albedo that is independent of location on the surface. It is nevertheless possible to apply the equation to a real case, where the albedo is horizontally inhomogeneous, if the horizontal scale of the adjacency effect is small compared to the horizontal scale of the albedo variation. This is true for optical depths less than ~0.75 when the scale of the adjacency effect is less than 1.5–2.0 km (Mekler and Kaufman, 1980).

Many natural surfaces have a non-Lambertian component in their bi-directional reflectivity function. Our approach, on the other hand, is based on the existence of a Lambertian albedo. While this may be a serious problem in some instances, it will not invalidate the present treatment as the non-Lambertian component is usually not important for many natural land surfaces, except for solar zenith angles larger than 60° (Kriebel, 1979).

In addition to being dependent on the surface albedo, the intensity measured from the satellite depends on the solar position in the sky as well as on the unknown optical depth, δ at the time of observation.

In order to determine the surface albedo under such conditions, we make the following approxima-

[1] Affiliated with Department of Meteorology, University of Maryland, College Park, MD 20742, and Goddard Laboratory for Atmospheric Sciences, NASA/GSFC, Greenbelt, MD 20771

tion to Eq. (1). For the case of A not close to one, Eq. (1) may be approximated by a polynomial of second order, $I^{A'}$,

$$I^{A'} \approx I^0 + GA(1 + LA) \equiv I^0 + aA + bA^2, \quad (2a)$$

where

$$a = G, \quad (2b)$$

$$b = GL. \quad (2c)$$

We consider the three functions I^0, a and b as empirical parameters.

The quantity LA in the denominator of the second term of Eq. (1) is the multiplication of the average diffuse reflectivity of the atmosphere L and the surface albedo, A. Both parameters are less than one. For the optical depths considered in this study, $L \ll 1$ [See discussion following Eq. (3)].

The great advantage and utility of this approach is that the determination of these three parameters may be done completely empirically without any prior knowledge at all of either the atmospheric optical properties or those of the satellite system. If one knows the surface albedo at three points in any given spectral image from independent measurements, one may solve Eq. (2) for I^0, a and b. These may then be used to construct a surface albedo map of the entire image.

The error in the approximation may be assessed as follows.

For any value of the surface albedo, the polynomial approximation leads to an intensity $I^{A'}$ instead of I^A. The relative deviation d of $I^{A'}$ from I^A must be smaller than the experimental error d_0, i.e.,

$$d_0 \geqslant d = \frac{I^A - I^{A'}}{I^A}, \quad (3a)$$

or

$$A^3 + \frac{(I^0L - G)}{GL^2} d_0A - \frac{I^0d_0}{GL^2} \leqslant 0. \quad (3b)$$

Values of I^0, G and L were computed for a reasonably inclusive array of aerosol models (Table 1) by the use of a radiation code available at NASA–GSFC/GLAS (Y. Kaufman, 1981, private communication). The results are given in Table 2. It is obvious that they are not very sensitive to the exact aerosol model. For the remainder of our analysis, we therefore use an aerosol model 1 with an albedo for single scattering, $\tilde{\omega}_0$, of 0.976 and relative humidity of 70%. The experimental error d_0 is specified in the LANDSAT Data Users Handbook at ~3%.

The expression of (3b) with this value of d_0 and the equality sign is a cubic in A. The roots of this equation give the limits of A within which the inequality (3b) is valid. For the range

$$A_3 < A < A_1,$$

inequality (3b) is valid.

It is obvious that the range of A which is of interest in our context

$$0 \leqslant A \leqslant 1$$

is included in the interval (A_1, A_3). The real roots of the equality for our aerosol model are shown in Table 3. For all optical depths less than 0.75, the table may be used to show the inequality (3) to be valid for all values of A between 0 and 1. Higher optical depths are only rarely obtained in nature and would preclude in any case, the derivation of acceptable accurate values for the surface albedo (see Appendix).

The results of a similar analysis, for the other aerosol models are almost identical, indicating the applicability of the present approximation to a range of possible aerosol models.

3. The spectrally integrated intensities at satellite altitude

The spectrally integrated intensity measured by a satellite sensor is

$$I = \int_{\lambda_1}^{\lambda_2} I(\lambda) d\lambda, \quad (4)$$

where λ_1 and λ_2 are the wavelengths defining the limits of the various LANDSAT channels.

In terms of our approximation, Eq. (2) and Eq. (4) the integrated intensity may be written for each spectral interval

TABLE 1. Aerosol models with log-normal size distribution.*

Model	$\ln\sigma$	$\ln r_m$	n	k	g	$\tilde{\omega}_0$	RH (%)
1	0.6850	−3.11	1.43	0.0035	0.67449	0.97578	70
2	0.68824	−2.87	1.40	0.0023	0.71337	0.98355	80
3	0.69149	−2.63	1.36	0.0012	0.75226	0.99132	90
4	0.69311	−2.51	1.35	0.0006	0.77170	0.99520	95

* Definitions

σ width of size distribution
r_m mean radius of size distribution
n real part of refractive index
k imaginary part of refractive index
g anisotropy factor
$\tilde{\omega}$ albedo for single scattering
RH relative humidity.

TABLE 2. Radiative parameters of the atmosphere.*

			Aerosol model 1			
δ	0.0	0.250	0.500	0.750	1.000	2.000
I_λ^0	0.02170	0.03405	0.04766	0.06087	0.07349	0.11430
L	0.07943	0.13796	0.18203	0.21864	0.25361	0.35955
G	0.39990	0.34971	0.30750	0.27124	0.24093	0.15618
			Aerosol model 2			
δ	0.0	0.250	0.500	0.750	1.000	2.000
I_λ^0	0.02170	0.03186	0.04355	0.05535	0.06684	0.10640
L	0.07943	0.13068	0.17363	0.21126	0.24074	0.33865
G	0.39990	0.35845	0.32122	0.28965	0.26262	0.18453
			Aerosol model 3			
δ	0.0	0.250	0.50	0.750	1.000	2.000
I_λ^0	0.02170	0.03080	0.04111	0.05183	0.06247	0.10060
L	0.07943	0.13152	0.17405	0.20527	0.23135	0.31580
G	0.39990	0.36286	0.32976	0.30119	0.27635	0.20337
			Aerosol model 4			
δ	0.0	0.250	0.500	0.750	1.000	2.000
I_λ^0	0.02170	0.02985	0.03923	0.04890	0.05873	0.09503
L	0.07943	0.12850	0.16363	0.19796	0.22626	0.31008
G	0.39990	0.36682	0.33749	0.31063	0.28745	0.21870

* Zenith angle of upwelling radiation, 0°.
Zenith angle of incident radiation, 60°.
Solar constant, π units.

$$I^A = I^0 + \int_{\lambda_1}^{\lambda_2} G(\delta)d\lambda + \int_{\lambda_1}^{\lambda_2} G(\delta)A(\lambda)A^2(\lambda)d\lambda, \quad (5)$$

where $G(\delta)$ and $L(\delta)$ are functions of λ through the optical depth. Fig. 1 shows G, L, GL and I_0 as functions of δ for one of our aerosol models. The other models are not shown, as they give very similar results (Table 2). The three functions G, L and GL, may be approximated with good accuracy by the following expressions:

$$G = 0.282\delta^{-0.190}, \quad (6a)$$

$$L = 0.210\delta^{0.055}, \quad (6b)$$

$$GL = 0.059\delta^{-0.135}. \quad (6c)$$

The optical depth, δ, of atmospheric aerosols may increase, decrease or even peak with λ (e.g., Volz,, 1956; Angstrom, 1964; Joseph *et al.*, 1973; Levin *et al.*, 1980). We shall assume here for simplicity that

$$\delta = K\lambda^{-\gamma}, \quad -1 \leqslant \gamma \leqslant 2. \quad (7)$$

TABLE 3. The real roots of the error equation [Eq. (3)].

	Three real roots				One real root	
δ	0.0	0.25	0.50	0.75	1.0	2.0
A_1	2.2100	1.2900	1.0098	0.8698	0.7818	0.6498
A_2	−2.1600	−1.1940	−0.8440	−0.6000		
A_3	−0.055	−0.0880	−0.1656	−0.2698		

The range of γ assumed is significantly broader than the values usually encountered in the atmosphere.

The variations of G and GL over the spectral range of LANDSAT have been calculated using Eqs. (6) and (7) for different values of γ and are shown in Table 4. It is clear that in all spectral bands G and GL are practically independent of the wavelengths of the range of γ's chosen. Hence, with an accuracy of a few percent, we may express the integrated intensity I^A as

$$I^A = I^0 + \bar{a}\bar{A} + \bar{b}\overline{A^2}, \quad (8a)$$

where

$$\bar{a} = G(\Delta\lambda)(\lambda_2 - \lambda_1), \quad (8b)$$

$$\bar{b} = \mathrm{GL}(\Delta\lambda)(\lambda_2 - \lambda_1), \quad (8c)$$

$$\bar{A} = \frac{1}{\lambda_2 - \lambda_1}\int_{\lambda_1}^{\lambda_2} A d\lambda, \quad (8d)$$

$$\overline{A^2} = \frac{1}{\lambda_2 - \lambda_1}\int_{\lambda_1}^{\lambda_2} A^2 d\lambda. \quad (8e)$$

The occurrence of $\overline{A^2}$ is inconvenient. However, within a LANDSAT band, the difference between $\overline{A^2}$ and $(\bar{A})^2$ is not large—as will be shown below. In addition, the third term in Eq. (8a) is smaller than the second term [see Eq. (6)] so that its treatment may be less accurate.

Let us assume therefore in treating the third term that in a given spectral band, the surface albedo varies linearly with wavelength

$$A(\lambda) = \bar{A} + C(\lambda - \bar{\lambda}).$$

Then $\overline{A^2}$ in Eq. (8a) is given by

$$\overline{A^2} = \int_{\lambda_1}^{\lambda_2} \frac{A^2(\lambda)d\lambda}{\lambda_2 - \lambda_1} \approx \int_{\lambda_1}^{\lambda_2} [\bar{A} + C(\lambda - \bar{\lambda})]^2 \times \frac{d\lambda}{\lambda_2 - \lambda_1} = \overline{A^2}[1 + \tfrac{1}{3}(C/\bar{A})^2(\bar{\lambda}^2 - \lambda_2\lambda_1)]. \quad (9)$$

The largest variations of the albedo may be in the spectral interval 0.8–1.1 μm where a factor of 2 is possible over vegetation and $C\bar{A}^{-1}$ is then also of order 2.

For this case, the second term in the square brackets is 0.015 and thus the asumption $\overline{A^2} = \bar{A}^2$ leads to only a small error. The third term of the intensity equation (8a), the only one affected by this approximation, is always much smaller than the other two, for the case $\lambda_2 = 1.1$, $\lambda_1 = 0.8$,

$$\frac{\bar{b}\overline{A^2}}{\bar{a}\bar{A}} = 0.209\delta^{0.055}\bar{A}(1 + 0.015).$$

For the largest applicable optical depth, 0.75 and an unrealistically large albedo of 1, one gets the ratio to be 0.21. Usually, it will be much smaller.

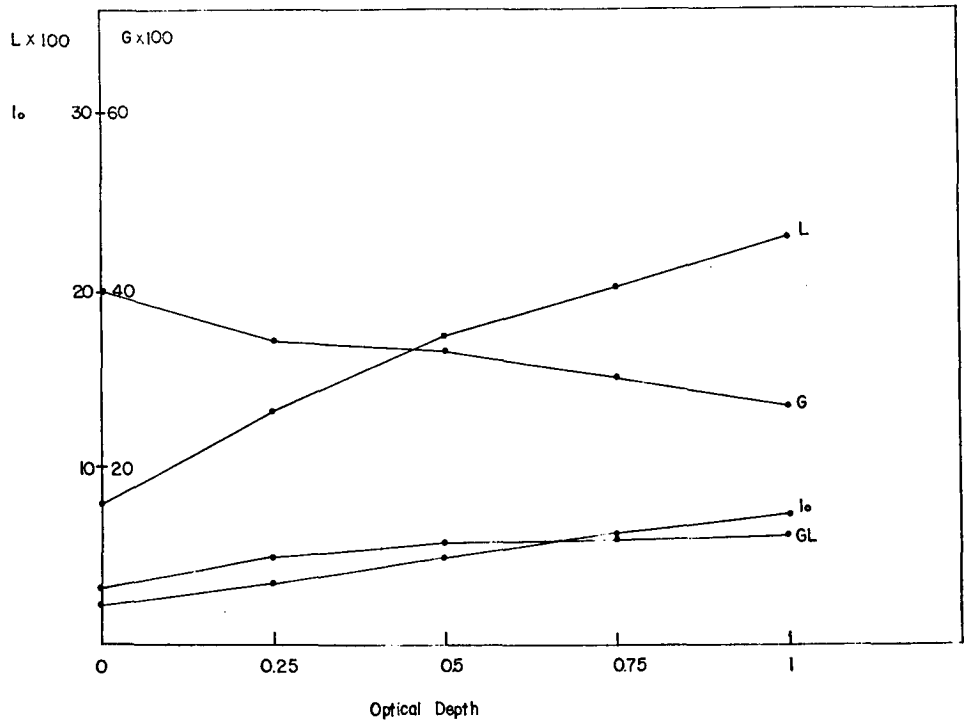

FIG. 1. Variation of I_0, G, L and GL with optical depth. Note separate scale for G.

The same analysis may be carried out for other dependences of the surface albedo on λ, the wavelength, with similar conclusions. One may therefore approximate the intensity in the following convenient manner:

$$I^A = I^0 + \bar{a}\bar{A} + \bar{b}\bar{A}^2. \tag{10}$$

4. Experimental determination of I^0, $\bar{a}$, $\bar{b}$

If one knows the surface albedo at three points in any spectral image from independent measurements, one may solve Eq. (10) for the constants I^0, $\bar{a}$ and $\bar{b}$.

Since I^0, G and L that go into the above constants are all functions of the optical depth δ this approach is equivalent to assuming that δ is constant over the LANDSAT image that is being analyzed.

The validity of this assumption was checked by an analysis of the possible relative error in the albedo $\delta A/A$ determined at a given point, different from the three used for finding the constant values of I^0, $\bar{a}$ and $\bar{b}$. The procedure is described in detail in the Appendix and summarized in Table 5.

The conclusion that may be drawn from Appendix 1 and Table 5 is that for all values of optical depth less than 0.75, the surface albedo less than 0.5, the relative error induced by our assumption is very small compared to 1.

The calibration points should be chosen such that the local albedos are stable and independent of season. The three points selected for our present purpose are in the desert in regions with little rainfall and no vegetation. One point is in the sandy area near Yamit in the Sinai Desert (31°13′N, 34°10′E), the other two near Mizpe-Ramon in the High Negev Desert of

TABLE 4. The spectral variation of G and GL in the LANDSAT bands.

λ_1/λ_2 (μm)	0.5/0.6	0.6/0.7	0.7/0.8	0.8/1.1
	(a) $G(\lambda_1)/G(\lambda_2)$			
$\gamma = -1$	1.0352	1.0297	1.0257	1.0624
0	1.0000	1.0000	1.0000	1.0000
1	0.9660	0.9711	0.9749	0.9413
2	0.9331	0.9431	0.9505	0.8860
	(b) $GL(\lambda_1)/GL(\lambda_2)$			
$\gamma = -1$	1.0249	1.0210	1.0182	1.0439
0	1.0000	1.0000	1.0000	1.0000
1	0.9757	0.9794	0.9821	0.9579
2	0.9520	0.9592	0.9646	0.9176

TABLE 5. The relative error in the albedo $\delta A/A$.

	δ					
A	0.0	0.25	0.50	0.75	1.0	2.0
0.05	−0.019	−0.0540	0.0827	0.1044	0.1226	0.1782
0.10	−0.019	0.0175	0.0318	0.0427	0.0518	0.0796
0.20	−0.019	−0.0008	0.0064	0.0119	0.0164	0.0303
0.40	−0.019	−0.0099	0.0063	−0.0036	−0.0013	0.0057

Southern Israel (30°33′N, 34°40′E; 30°36′N, 34°46′E). These points also appear on all LANDSAT images of the southern part of the country. In addition, one may use water surfaces or jungle-type vegetation.

A spectrophotometer with an integrating sphere was built for the purpose of measuring the local surface albedo. The instrument is described in Fig. 2. It is equipped with seven interference filters of 100 μm width each, which cover all spectral bands of LANDSAT. There are two detectors—a photo diode for the visible part and a photo-resistor for the IR part of the solar spectrum. Measurements were made for two positions of the instrument—right side up and inverted.

The ratio of the second to the first flux gives the local albedo. The instrument was elevated to ~2.5 m to preclude shadowing effects. The measurement areas were chosen to be homogeneous over the whole field of view of the integrating sphere (2π). The results of the measurements are given in Table 6 and Fig. 3. The Yamit point shows a very high spectral albedo, the Negev (one) point is about average and the Negev (two) has a very low albedo. The derived parameters I_0, $\bar{a}$ and $\bar{b}$ should thus be applicable to a wide range of surface albedos.

The choice of location and the measurement of the albedo have been described in detail in this Section. The reasons are that stable and correct values of the albedo at the three reference points are crucial to the success of any application of the present method. The actual application will be given in a subsequent paper.

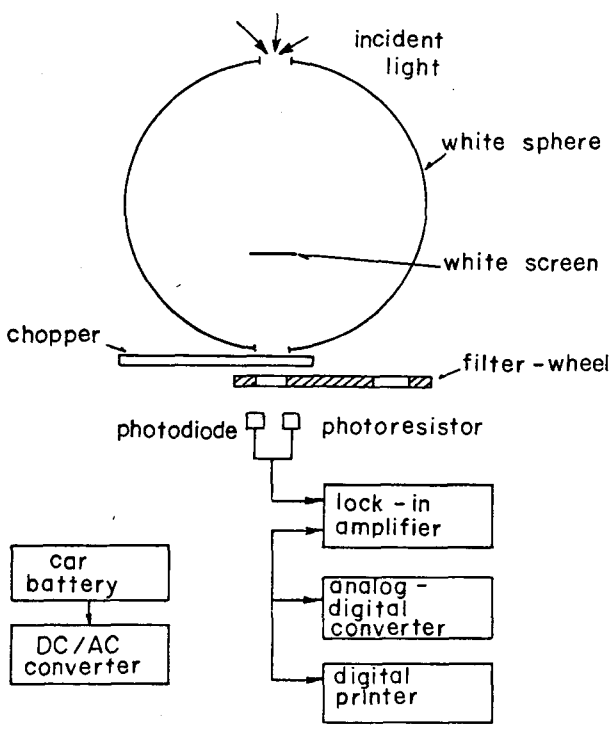

FIG. 2. Schematic diagram of integrating sphere spectro-radiometer.

TABLE 6. Measurements of spectral albedo at three locations.

λ (Å)	Yamit*	Negev** (one)	Negev*** (two)
4500	0.45	0.10	0.05
5500	0.60	0.11	0.05
6500	0.67	0.11	0.05
7500	0.72	0.14	0.06
8000	0.75	0.20	0.08
9000	0.75	0.23	0.09
10000	0.79	0.30	0.11

* Yamit quartz sand.
** Negev (one) Cenomanian Dolomite limestone.
*** Negev (two) Lower Cretaceous basalt.

5. Application to satellite data

The determination of the three constants in the equation for the intensity may be done from knowledge of the optical depth and the properties of the observing system as outlined in the previous sections, given the three independently known surface albedos and intensities at a given time.

It is however advantageous to treat the constants as instrumental parameters and determine them empirically for each individual image in a given spectral interval.

One may write three equations:

$$I_1 = I_0 + \bar{a}A_1 + \bar{b}A_1^2,$$

$$I_2 = I_0 + \bar{a}A_2 + \bar{b}A_2^2,$$

$$I_3 = I_0 + \bar{a}A_3 + \bar{b}A_3^2,$$

the solution of which for I_0, $\bar{a}$ and $\bar{b}$ is immediate. If the albedos that are independently measured are quite different, the parameters will be useful over the whole possible range of albedo and the set of equations will be solvable.

6. Summary and conclusions

Starting with the exact solution for the upwelling intensity from a turbid atmosphere overlying a surface with a homogeneous Lambertian albedo, we have developed a technique for the derivation of the spectral surface albedo of regions with a minimum size of ~(2–4) × 10^6 m^2.

The assumptions under which the theory is valid are that the optical depth of the atmosphere be less than 0.75, that the latter be constant over the field of view and that the deviation from a Lambertian albedo is small.

The restriction to optical depths less than 0.75 is not serious, in our opinion, because higher optical depths are not usually found and would preclude a reliable measurement of the surface albedo in any case.

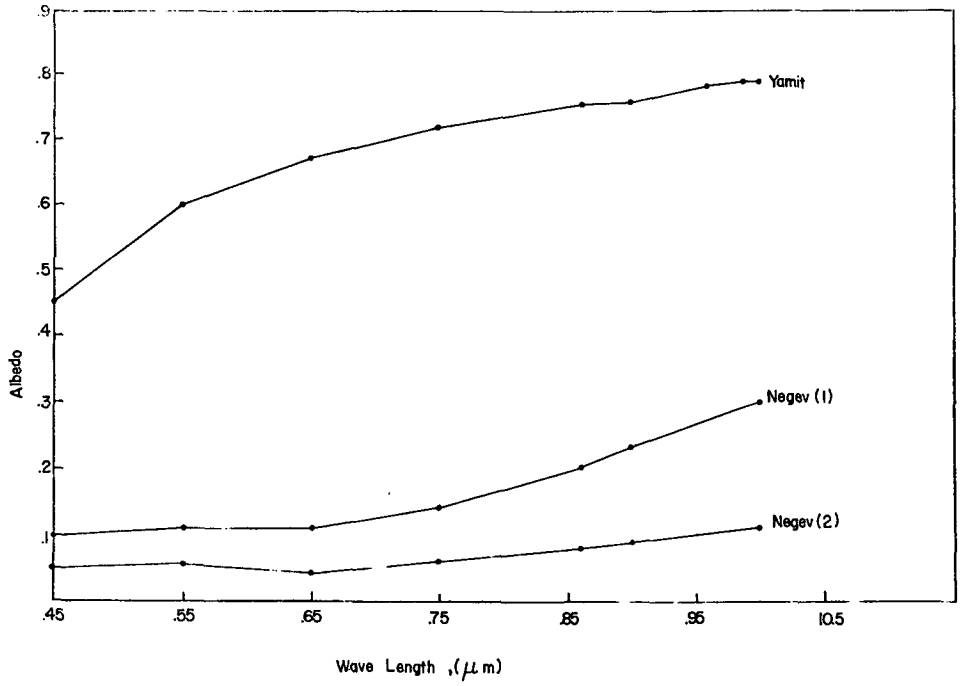

FIG. 3. Spectral variation of measured albedos.

The assumption that the optical depth, while generally less than 0.75, does not vary over the field of view has been shown not to introduce relative errors in the determination of the albedo larger than 10%. Any fluctuations in the relative optical depth $\Delta\delta/\delta$ larger than those assumed in the analysis, 0.1, would be discernible in the imagery.

Even the existence of thin "invisible" cirrus aloft would not invalidate our suggested approach if the cloud layer is reasonably homogenuous. The reason is the complete independence on any data, except for intensity and albedo at some points in the FOV.

Whenever it is impossible to measure a very high albedo as part of the reference data, one may, with slightly lower accuracy use a linear approximation to Eq. (1) instead of the parabolic one used here. There would be little error in regions of low to medium albedo. If it is impossible to measure reference albedos at temporally stable sites, one may accumulate seasonal data at suitable points. If even that is impossible, or the reference points are masked by clouds, one can fall back upon the conventional methods now in use.

The great advantage to the present approach is that it is possible to apply this technique to any image in which the albedo is independently known at at least three or even two points. The optical properties of the atmosphere and of the satellite system need not be known. Under such circumstances, the parameters of fit for our approximation can be uniquely determined *for each separate satellite-image* and an albedo map can be produced in each spectral band. It is our opinion that the inherent simplicity of the present approach outweighs the limitations in the assumptions.

Applications of this technique are numerous and some will be published in subsequent publications.

Acknowledgments. We would like to thank Dr. Y. Kaufman for calculations of the upwelling intensities as well as for the measurement of the three surface albedos. We are grateful to Mr. Boris Strobinats for efficient structure and maintenance of the spectrophotometer. Mrs. Zahava Barokas drafted the figures and Mrs. Rachel Duani typed the manuscript.

Three anonymous referees produced thoughtful and informative comments which resulted in significant improvements in both content and presentation of our paper.

APPENDIX

Investigation of the Assumption that the Aerosol Optical Depth is Constant Throughout the Image

Let the functions $I_0(\delta)$, $G(\delta)$ and $GL(\delta)$ at a given point be different from those at the three reference points. The intensity at satellite altitude from that point with true albedo A_t and optical depth δ is

$$I^A = I_t^0 + G_t\bar{A}_t + (GL)_t\bar{A}_t^2. \quad \text{(A1)}$$

The same intensity I^A, however, is modelled by

$$I^A = I_e^0 + G_e\bar{A}_e^2 + (GL)_e\bar{A}_e^2. \quad \text{(A2)}$$

The difference between these two equations relates the error in the albedo with the error in the optical depth. The first step in the analysis is the simplification of the two equations by neglecting the last term in each. This is permissible as shown in our paper.

From the difference between Eqs. (A1) and (A2) one may then derive the error in the albedo

$$\delta\bar{A} = \frac{I_e^0 - I_t^0}{G_t} + \frac{G_e - G_t}{G_t} A_e. \qquad \text{(A3)}$$

We approximate the differences $I_t^0 - I_e^0$ and $G_t - G_e$ by

$$I_t^0 - I_e^0 = \frac{\partial I_t^0}{\partial \delta} \Delta\delta, \qquad \text{(A4a)}$$

$$G_t - G_e = \frac{\partial G_t}{\partial \delta} \Delta\delta. \qquad \text{(A4b)}$$

The values of the derivatives are taken from our analytical approximations to I^0 and G (see text) and consequently, one may derive

TABLE A1. Albedo relative error, $\delta\bar{A}/\bar{A}$ versus A and δ.

	δ				
A	0.25	0.50	0.75	1.0	2.0
0.05	−0.15	−0.04	0.05	0.12	0.36
0.10	−0.07	−0.02	0.02	0.06	0.18
0.20	−0.04	−0.01	0.01	0.03	0.09
0.40	−0.02	−0.01	0.01	0.02	0.05

$$\frac{\delta\bar{A}}{\bar{A}} = \frac{\Delta\delta}{\delta\bar{A}} (0.2514\delta^{0.554} - 0.19). \qquad \text{(A5)}$$

We assume that the relative error in the optical depth, $\Delta\delta/\delta$, is O(0.1). The presence of larger irregularities would be obvious in the image for all detectable optical depths, $\delta > 0.25$ (e.g. Kaufman and Joseph, 1981) and such points would not be treated with our present scheme.

The relative error in the albedo is given in Table A1 as a function of optical depth of the aerosol and albedo. It is obvious from the size of the relative error that the assumption of constant δ is acceptable for optical depths between 0.25 and 0.75.

REFERENCES

Angstrom, A., 1964: The parameters of atmospheric turbidity. *Tellus*, **16**, 64–75.

Chandrasekhar, S., 1960: *Radiative Transfer*, Dover, 393 pp.

Joseph, J. H., A. Manes and D. Ashbell, 1973: Desert aerosols transported by Khamsimic depressions and their climatic effects. *J. Appl. Meteor.*, **12**, 792–797.

Kaufman, Y., and J. H. Joseph, 1981: Evaluation of surface albedo and extinction characteristics of the atmosphere from satellite images. *J. Geophys. Res.*, **87**, 1287–1299.

Kriebel, K. T., 1979: Albedo of vegetated surfaces: Its variability with differing irradiances. *Remote Sens. Environ.*, **8**, 283–290.

Levin, Z., J. H. Joseph and Y. Mekler, 1980: Properties of Sharav (Khamsin) dust-comparison of optical and direct sampling data. *J. Atmos. Sci.*, **37**, 882–889.

Mekler, Y., and Y. Kaufman, 1980: The effect of Earth's atmosphere on contrast reduction for a non-uniform surface albedo and two-halves field. *J. Geophys. Res.*, **85**, 4067–4083.

Sobolev, V. V., 1975: *Light Scattering in Planetary Atmospheres*. Pergamon Press, 450 pp.

Volz, F., 1956: Optik der Tropfen, *Handbuch der Physik*, Vol. VIII, Springer Verlag, 80 pp.